

Aspects of the Photodimerization Mechanism of 2,4-Dichlorocinnamic Acid Studied by Kinetic Photocrystallography[†]

J. Davaasambuu, G. Busse, and S. Teichert*

Max-Planck-Institut für biophysikalische Chemie, Abteilung Spektroskopie und Photochemische Kinetik, Am Fassberg 11, 37077 Göttingen, Germany

Received: August 22, 2005; In Final Form: December 12, 2005

Photoinduced structural variations in single crystals of 2,4-dichloro-trans-cinnamic acid (C₉H₆Cl₂O₂, DiClCA) have been investigated using X-ray diffraction (photocrystallography) and optical spectroscopic methods. During UV irradiation, which initiates the irreversible dimerization reaction, a loss of the long-range order of the reactant single crystal was found, i.e., that the dimerization is a heterogeneous one. This unexpected result emphasizes the still-existing problem of predicting changes or of remaining periodicity during chemical reactions in the solid state. On the basis of the experimental results, we propose a qualitative kinetic reaction scheme for DiClCA heterogeneous dimerization reaction.

Introduction

Photoinduced processes in organic single crystals have been studied for a long time, and in recent years their potential for possible technical applications in a variety of photosensitive devices made them the focus of research.^{1–3} In synthetic chemistry, template-controlled reactions in the organic solid state can be used to construct a molecule that functions as an organic building unit of both a metal–organic polyhedron and polygon.⁴ In this way, it is possible to simulate two-step processes which consist of a template-directed synthesis step and a self-assembly step in order to construct large, functional self-assembled structures. Photoinduced solid-state reactions are ideal for initiating at least one of these steps.

From a general kinetic point of view, photoinduced solid-state reactions^{5–27} can be separated into two categories: reversible and irreversible reactions. The formation of optically created short-living transient structures or intermediates that finally direct the reaction pathway is a common feature for both.^{5–10} The structure of these intermediates can be investigated by time-resolved laser-pump/X-ray-probe experiments as they are provided by time-resolved X-ray diffraction techniques. The short-pulsed X-rays are either generated by plasma sources in laboratories or provided as brilliant picosecond X-ray pulses at today's synchrotron sources. So far, most reactions studied by time-resolved X-ray diffraction make use of the repetitive character of the pump/probe experiment and are of reversible nature, whereas most photodimerizations^{7,11–19} in single crystals are irreversible reactions, i.e., the resulting product structures remain.

In the solid state, two kinds of dimerization reactions can be distinguished: homogeneous single-crystal to single-crystal dimerization and heterogeneous dimerizations where the long-range order is destroyed. Depending on the optical excitation conditions, the same kind of photodimerization can be homogeneous or heterogeneous.^{14,15} Time-resolved X-ray diffraction is a unique and powerful method to distinguish between these

different reactions since crystallography probes the structural rearrangements of the *bulk* under illumination.^{7,25} In contrast, spectroscopy gives evidence of the *local* structural changes.

The mechanism of photodimerization is explained by the so-called topochemical principle. Since their first introduction in 1931,²⁰ topochemical reactions in the crystalline state have been a permanent topic of experimental studies in different solid-state schools.^{11–27} Crystal systems, which follow the topochemical principle, undergo a [2 + 2] photodimerization,²² if the reactants pack in a molecular mode with intermolecular double bond distances of $r < 4.2$ Å. Crystal modifications of the same chemical species with intermolecular double bond distances $r > 4.2$ Å are photoinactive. Thus photoactivity does or does not occur depending on the chromophore packing. The photoactive morphologies are further distinguished between so-called α -type crystals, where the chromophores stack in opposite directions such as head–tail \leftrightarrow tail–head leading to centrosymmetric products, and β -type crystals, where the chromophores order in a parallel way to head–tail \leftrightarrow head–tail forming mirror-symmetric products.

On the basis of these initial characterizations of crystal-packing properties of organic solids and their influences on crystal reactivity, up to now permanent progress has been made in order to come to a more detailed and quantitative mechanistical picture of organic photochemistry in crystal lattices.^{23–25} In particular the progress in the theoretical models coupled with the increase of computer simulation capabilities makes it now possible to simulate lattice-dictated solid-state reactions on a high level ab initio quantum mechanic/molecular mechanic approach. The simulations enable an accurate mechanistical description, e.g., of photoinduced type-B rearrangements as they can be photoinduced in bicyclo-hexen-ones derivatives in a homogeneous crystal reaction.²⁵

Pure molecular mechanic simulations themselves have been used in order to describe the role of cage effects, local stress, and friction (in the form of hindered rotations) on the photo-reaction of crystalline benzoyl peroxide dissociation.²⁶

By going back to the early work of Cohen and Schmidt and their concept of reaction cavity, chromophores in crystals can be visualized as existing in rigid, three-dimensional cavities

[†] Part of the special issue "Jürgen Troe Festschrift".

* To whom correspondence should be addressed. E-mail: stecher@gwdg.de.

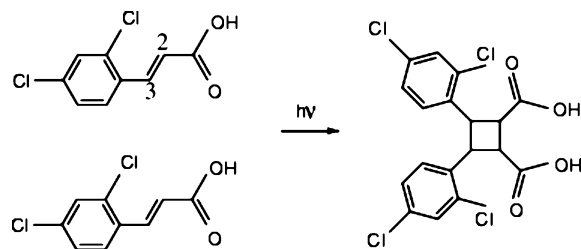


Figure 1. Reaction scheme of the [2 + 2] photodimerization in DiCICA.

formed by their nearest neighbors.^{16,27} As the central molecule reacts, its geometry changes within the cavity. Reactions that involve minor changes in reactant geometry are topochemically allowed, since they progress without restriction from the cavity walls. Reactions with transition-state geometries that do not fit within the cavity are strongly disfavored.

The influence of this special feature of solid-state reactions which lead to the mentioned formulation of the “reaction cavity”, meaning the influence of “available cavity space” in the crystal lattice with respect to the particular molecular volume, has furthermore been studied for organic solid-state reaction in refs 28 and 29.

From an energetic point of view, the role of attractive and repulsive van der Waals forces on the energies of the reactant and product states, respectively, has intensively been investigated in ref 30.

The aim of this work is to present some more detailed spectroscopic and photocrystallographic investigations on the mechanism of a recently reported topochemical reaction of single crystal 2,4-dichloro-*trans*-cinnamic acid (DiCICA).³¹ Figure 1 presents the suggested reaction scheme of the [2 + 2] photodimerization in DiCICA single crystals, where two parallel double bonds of neighbor molecules form a cyclobutane ring under light irradiation.

On the molecular level, the evolution of photodimerization has been followed by infrared and UV/vis spectroscopy. The bulk phototransformation has been investigated by time-resolved X-ray diffraction that gives clear evidence of the morphological changes during photodimerization. The single-crystal structure of the monomer has been solved, and the time evolution of its structure has been studied and compared with the photoinduced short-range order changes, which were monitored with spectroscopic methods. Finally, the experimental results are explained within a generalized reaction scheme implementing possible homogeneous and heterogeneous reaction pathways in solid-state reactions.

Experimental Methods

DiCICA was purchased from Aldrich Chemical Co. For the X-ray diffraction experiments, single crystals of the photodimerizable β -form of DiCICA were grown from oversaturated acetic solution. For the IR and optical measurements, the DiCICA crystals were crushed and prepared as potassium bromide (KBr) pellets with 0.9 mm thickness and 13 mm diameter size.

For both the optical measurements and the X-ray diffraction experiments, the samples were irradiated with a high-pressure mercury lamp at the red tail of the absorption band at $\lambda_{\max} = 350$ nm.³² The light was transported to the sample via a fused silica fiber optic bundle (LINOS Photonics) and attenuated with a UG 11 filter and (optionally) a fuse plate. The measurements were performed at room temperature and at 132 K. For the

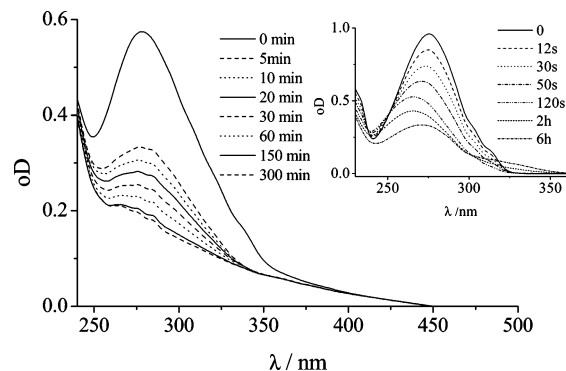


Figure 2. Changes of the optical absorption spectra as a function of illumination time. The dimerization can be followed by a decrease of the monomer band with a maximum at 275 nm. With a chromophore/photon ratio of 400, the kinetic analysis of the optical spectra yields a decay time of $\tau_1 = 12$ min for the reaction in the crystalline state. Inset: in contrast, photodimerization in methanol solution yields in the formation of a short and long living species $\tau_1 = 17$ s and $\tau_2 = 14$ 200 s).

optical measurements, the illumination power was about 0.2–0.5 mW/cm².

Under the same optical excitation conditions the photoinduced short-range structural variations in the crystals were monitored by infrared spectroscopy (with a Bruker IFS 25 FTIR spectrometer between 800 and 3500 cm⁻¹) and by optical absorption spectroscopy (with a Cary-5E spectrometer between 200 and 800 nm). For the optical absorption measurements, an empty KBr pellet was used as reference, and its spectrum was subtracted from the sample spectrum. The decrease of the optical spectra was fitted according to $\sum A_i \tau_i$ by means of a least-squares fitting method.

The mass spectra were determined with a Varian MAT CH7 mass spectrometer (EI, 70 eV).

Single-crystal X-ray diffraction was collected on a four-circle diffractometer with Mo K α radiation and a Bruker SMART charge-coupled device (CCD) as detector. The sample-to-detector distance was 48.7 mm. For the structure solution, DiCICA crystals of 0.5 × 0.2 × 0.1 mm³ size were chosen. The crystals were cooled with an open-flow N₂ gas stream. The diffraction patterns were integrated and corrected with the SAINT and SADABS programs.³³ The crystal structure of the monomer was solved by direct methods using the SHELXTL program package.³⁴

For the photocrystallographic studies, the crystal sizes varied between 0.5 × 0.2 × 0.1 mm³ up to 0.1 × 0.1 × 0.1 mm³. Also photo powder diffraction experiments were performed. For the photocrystallographic experiments an illumination power of 13 mW/cm² was required guaranteeing comparable illumination conditions to the optical experiments. It should be noted that, due to the extremely small single crystals, the effective illumination power on the sample was less than 5 mW/cm². Additional experiment with monochromatic excitation at $\lambda_{\max} = 420$ nm (3 mW/cm²) were undertaken to check the dependence of the dimerization on the excitation wavelength. The experiments were performed at room temperature and at 130 K.

Results and Discussion

To investigate the photodimerization of DiCICA on a molecular level, spectroscopic and analytical measurements were performed before, during, and after light irradiation. The changes in the optical absorption spectra during the photoreaction are summarized in Figure 2. It was found that the intensity of the

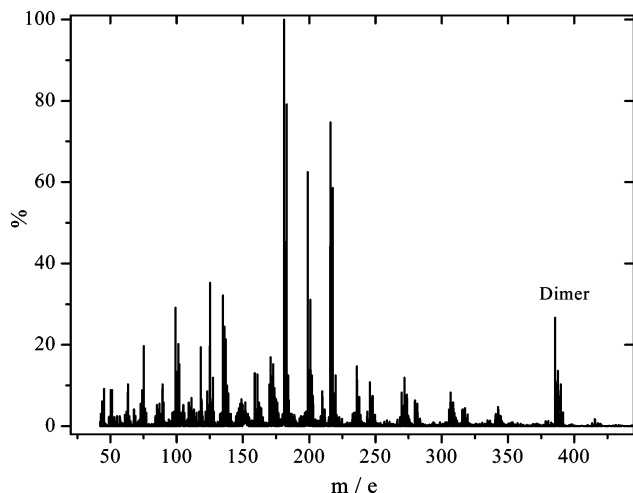


Figure 3. Mass spectrum of the product state of the photodimerization. In the spectrum for the illuminated sample, new peaks were observed near the mass-to-charge ratio of m/z (%) = 386 (20). The found mass belongs to a fragment where the Cl group and an OH group are split apart from the dimer product. The mass-to-charge ratio near m/z (%) = 216 (100) is explained as a remaining monomer due to an incomplete photoreaction.

monomer band with an absorption maximum at 275 nm decreases rapidly with progressing 350 nm light irradiation. For the dimerization reaction, the kinetic time law depends on the number of illuminated chromophores and the number of exciting optical photons. With a chromophore/photon ratio of 400, the kinetic analysis of the change in intensity of the optical spectra yields a decay time of $\tau_1 = 12$ min. By application of the Lambert–Beer law, the decrease of the monomer concentration is shown as normalized correlation function in Figure 6.

In contrast, photodimerization in methanol solution yields in the formation of a short and long-living species (shown as inset in Figure 2). Under excitation conditions comparable to those in the single crystals, two intensity decay times of the monomer absorption band with $\tau_1 = 17$ s and $\tau_2 = 14$ 200 s were found. The absorption spectra of DiCICA in methanol do not only show an intensity decrease of the reactant absorption but also a shift of the first absorption band maximum from 276 to 262 nm within 110 s followed by a red shift to 272 nm during 75 100 seconds (which is another measure of the same reaction to another photoproduct). We interpret this behavior as a second photoreaction—probably a photoelimination of Cl from the chromophore—which is enhanced in solution compared to the crystal. This is also supported by the results of the mass spectra presented below.

Infrared analysis of the photodimerization essentially reproduces the results reported in ref 31: with increasing illumination the maxima of the vibrational stretching band $\nu(\text{C}2=\text{C}3)$ at 1619 cm^{-1} decrease due to the breaking of the C2=C3 double bond in the molecules (spectra are not shown). As a result of the change in the chemical environment, the $\nu(\text{C}=\text{O})$ stretching mode at 1690 cm^{-1} shifts to higher energies that are typical for the dimer product. This shift might also be caused by an internal stress in the lattice created upon photoexcitation and proceeding reaction, as been reported in ref 26.

The mass spectrum of the product state of the photodimerization is shown in Figure 3. In the spectrum for the illuminated sample, new peaks were observed near the mass-to-charge ratio of m/z (%) = 386 (20). The mass found belongs to a fragment where the Cl group and an OH group are split apart from the dimer product. The mass-to-charge ratio near m/z (%) = 216 (100) is explained as remaining monomer due to an incomplete

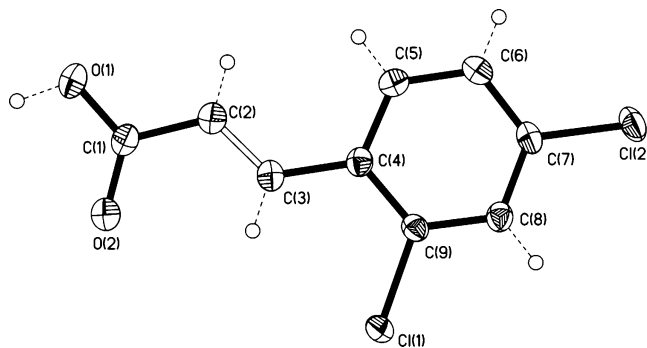


Figure 4. The monomer structure of DiCICA as determined through single-crystal diffraction. The phenyl ring within the monomer is almost planar with respect to the dimerizing double bond. The intermolecular distance between the C=C double bonds was found to be 3.813 Å fulfilling the topochemical criterion. It should be noted that the molecular long axis is not parallel to a crystallographic axis. All geometrical parameters including the isotropic and anisotropic temperature factors are listed in Table 1 and Table 2 of Supporting Information.

photoreaction. The results are an independent evidence of the photodimerization.

The long-range order changes in this photodimerization reaction were investigated by time-resolved X-ray diffraction. DiCICA monomer crystallizes in the triclinic space group **P-1**.³⁵ The monomer structure was determined in detail and refined by the full-matrix least-squares methods to a final R-factor of 3.3%. The molecular structure is shown in Figure 4. Its geometric parameters are listed in Tables 1 and 2 in Supporting Information (including the isotropic and anisotropic temperature factors).

The intermolecular distance between the C=C double bonds was found to be 3.813 Å fulfilling the criterion of a topochemical reaction ($r(\text{C}=\text{C}) < 4.2$ Å). The phenyl ring is almost planar with respect to the double bond. It should be noted that the molecular long axis is not parallel to a crystallographic axis.

Though the crystals were optically excited in the red shoulder of the absorption band with low fluences of excitation light the time-resolved X-ray diffraction studies, surprisingly, lead to an amorphization during the photoreaction. The decrease of the diffraction intensity as a function of time is presented for some selected times in Figure 5. The X-ray diffraction measurements were performed on the same crystals. After 60 min of irradiation (5 mW at the sample), no diffraction pattern was observed anymore, and the heterogeneous photodimerization of DiCICA single crystal was completed. Variations of the experimental conditions, as they are lowering the sample temperature to 130 K, investigating the photodimerization for various crystal sizes (up to $0.1 \times 0.1 \times 0.1$ mm³), performing photo X-ray diffraction experiments and using 420-nm excitation light, yielded all in the heterogeneous product state.

The disappearance of the Bragg diffraction pattern is assigned to the breaking of the long-range order in the crystal into smaller units of product domains. The domains seem to be so small that even sharp powder rings of the product state are suppressed and only an increase of the broad background signal can be recognized. Therefore we conclude that the dimerization coincides with the loss of long-range order.

By application of the scheme suggested in ref 36 and a chromophore/photon ratio comparable to that for the reported absorption measurements (here 410), a decay time of $\tau = 3.5$ min has been refined. This kinetic X-ray diffraction decay time is on the same order of magnitude as the decay time resulting from the optical data for the same chromophore/photon ratio.

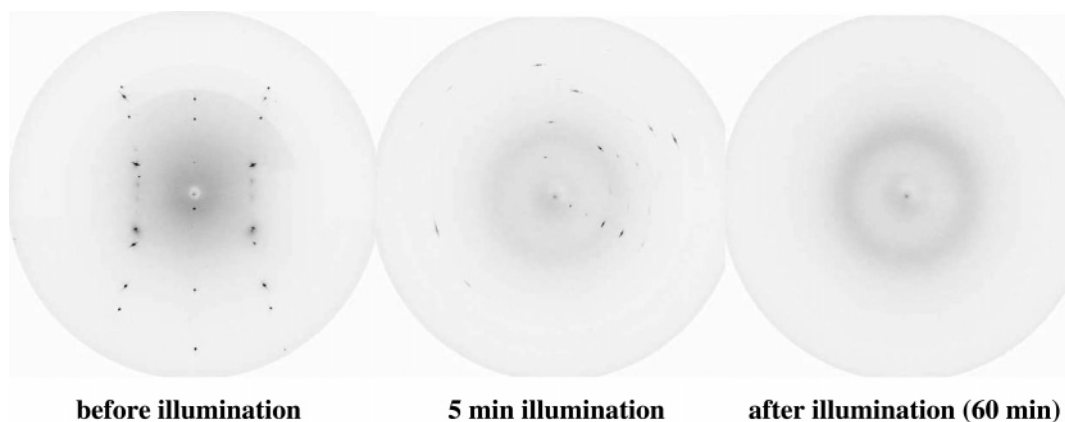


Figure 5. CCD snapshots of the DiCICA single-crystal diffraction under illumination suggesting a heterogeneous product formation.

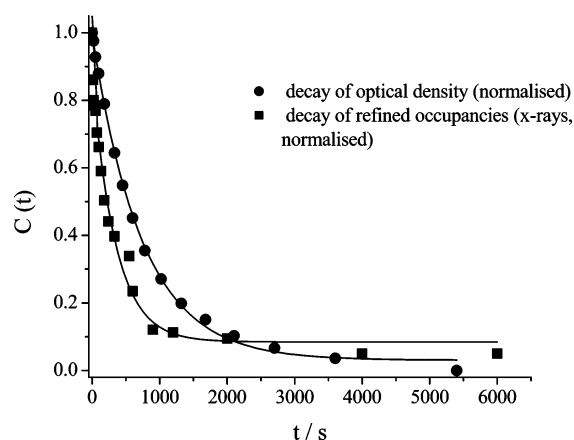
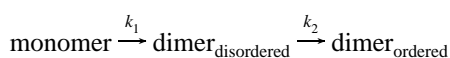


Figure 6. Comparison between the spectroscopic and the X-ray diffraction correlation functions of DiCICA photodimerization.

Both decay times are compared in Figure 6 as normalized correlation functions. Since the structure of the monomer was known it was possible to refine the number (or concentration) of diffracting monomer as a function of time and to correlate this concentration with the concentration changes derived from the optical experiments.

In recent years, considerable progress has been undertaken in order to describe more precise and in more mechanistical detail photochemical reactions in crystal lattices.^{23,25} Current effort from our side follows the theoretical route suggested in ref 25 and will be topic of future work.³⁷ Here, we therefore would like to concentrate in a first very qualitative approach of describing the experimental findings of a heterogeneous reaction in DiCICA. Figure 7 schematically summarizes the differences in the reaction path over the energy hypersurfaces for both reactions. The following simple reaction scheme can be suggested



In homogeneous reactions (solid line and dashed arrow in Figure 7), the reaction progresses from an ordered monomer state to an ordered dimer state via the formation of a disordered dimer state as an intermediate or metastable state. For the quasistationary case, $d[\text{dimer}_{\text{disordered}}]/dt = 0$. The population of the intermediate depends on the steepness of the $\text{dimer}_{\text{disordered}}$ species in the free-energy diagram and hence on the ratio k_1/k_2 or $\Delta G_1^\ddagger/\Delta G_2^\ddagger$, respectively. Note, that depending on the system $\Delta(\Delta G_1) \leq \Delta G_2^\ddagger$ or $\Delta(\Delta G_1) > \Delta G_2^\ddagger$ meaning that the energy maxima of the curve will vary.

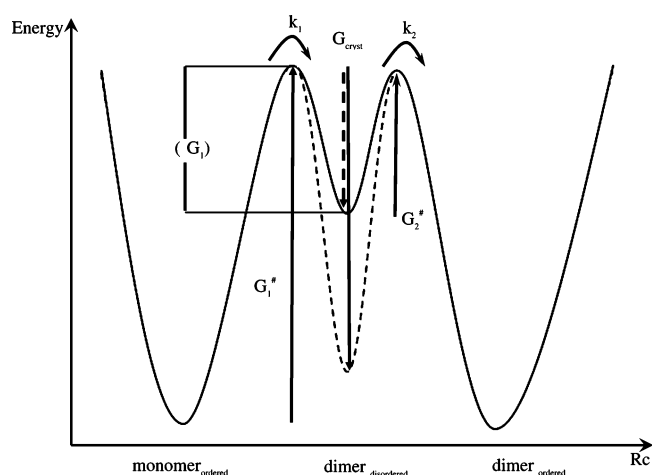


Figure 7. Reaction scheme of homogeneous and heterogeneous photodimerization reactions. In homogeneous reactions (solid curve, dashed arrow) the reaction progresses from an ordered monomer state to an ordered dimer state via the formation of a disordered dimer state as an intermediate or metastable state. The energy minimum of the $\text{dimer}_{\text{ordered}}$ state lowers as the reaction proceeds in the crystal. In heterogeneous reactions, the dimer disordered state is stabilized in such a way that the activation energy cannot be gained out of the energy available in the system. Now the disordered intermediate is a final product state and the crystals transform to this amorphous state (solid arrow, dashed curve). The population of the intermediate depends on the steepness of the $\text{dimer}_{\text{disordered}}$ species in the free-energy diagram and hence on the ratio k_1/k_2 or $\Delta G_1^\ddagger/\Delta G_2^\ddagger$, respectively. Note, that depending on the system $\Delta(\Delta G_1) \leq \Delta G_2^\ddagger$ or $\Delta(\Delta G_1) > \Delta G_2^\ddagger$.

In thermally supported photodimerizations, the activation energy over the second barrier is $\Delta G_2^\ddagger \approx kT$, thus allowing the crossing of the barrier from the disordered dimer state to the ordered dimer state under the experimental temperature conditions chosen. Also cooperative effects play in important role for the photodimerization as the energy minimum of $\text{dimer}_{\text{ordered}}$ state lowers as the reaction proceeds in the crystal. The sketched scheme might also explain some reported temperature dependences of photodimerizations as reported in ref 38.

For heterogeneous photodimerizations (dashed curve and solid arrow) the $\text{dimer}_{\text{disordered}}$ state is stabilized so that $\Delta G_2^\ddagger \gg \Delta G_1^\ddagger$ and $\text{dimer}_{\text{disordered}}$ is the final product state. Here, the photodimerization is of pseudo-first-order with $-d[\text{monomer}]/dt = d[\text{dimer}_{\text{disordered}}]/dt = k_1[\text{monomer}](t=0) \exp[-k_1 t] = k_1[\text{monomer}]$ and the crystal continuously transforms to the amorphous product state. For the reaction start ($t = 0$), the optically investigated reaction rate is $-d[\text{monomer}]/dt = 1.25 \times 10^{14}$ molecules/s in molecular units. The reaction rate investigated by kinetic X-ray diffraction is $d[\text{monomer}]/dt = 1 \times 10^{14}$

molecules/s (also for $t = 0$) guaranteeing a comparable molecule/photon ratio of 400 (to 410). The average rate constant is $k_1 = 3.1 \times 10^{-3} \text{ s}^{-1}$.

Though DiCICA was excited on the red tail of the absorption band, time-resolved X-ray diffraction evidences a heterogeneous mechanism for the photodimerization. Taking into account the crystallographic results in addition to the topochemical distance criterion of 4.2 Å,^{11,22} we suggest including other dimensions of the monomer configurations in the crystal lattice which probably also play a decisive role in the photodimerization reaction. Structurally one of the differences between the chromophore arrangement in homogeneous^{15,17,18} and heterogeneous^{19,22} photodimerization reactions is the extent of parallelism of the reacting C=C double bonds of two chromophores in the crystal lattice. In DiCICA the C=C double bonds span a small angle of 5° with respect to the crystallographic axis. To overcome the lack of parallelism, the chromophores have to rearrange during the photoreaction. Probably this rearrangement causes the formation of mosaic blocks, which are slightly displaced relative to each other and lead to a destruction of the long-range order as the reaction progresses through the crystal.

Conclusion

Kinetic analysis of the optical spectroscopic and the X-ray diffraction data of DiCICA upon UV excitation evidence a heterogeneous dimerization reaction. The crystal was photoexcited on the red tail of the absorption spectrum of the DiCICA monomer. The result observed was unexpected and emphasizes the still-existing problem of predicting changes or remaining of periodicity during chemical reactions in the solid state. Taking into account the crystallographic results, we suggest including other dimensions of the monomer configurations in the crystal lattice. In DiCICA, the C=C double bonds span a small angle of 5° with respect to the crystallographic axis. To overcome this slight lack of parallelism during the reaction, the chromophores have to rearrange during the photoreaction. Probably this rearrangement causes the formation of mosaic blocks and lead to a destruction of the long range order as the reaction progresses through the crystal. On the basis of the experimental results a simplified kinetic reaction scheme for homogeneous and heterogeneous reactions has been proposed. In this scheme, the disordered dimer state has some kind of intermediate character for homogeneous reactions. The energy of the final ordered product state lowers as the reaction proceeds in the crystal. In heterogeneous reactions the activation energy cannot be gained out of the energy available in the system and the crystals transform to the amorphous state.

To confirm and more precisely quantify the suggested reaction scheme in DiCICA, crystal simulations with high numerical precision and further spectroscopic and XRD investigations are performed. In our current effort, we follow the theoretical route suggested in ref 25 and this will be topic of future publications.

Acknowledgment. The authors thank Dr. M. Noltemeyer for his assistance with the single-crystal X-ray diffraction measurements. This work was supported by the Deutsche Forschungsgemeinschaft, Grant TE 347/1-3.

Supporting Information Available: Tables showing crystal data and structure refinement; atomic coordinates and equivalent

isotropic displacement parameters; and bond lengths, bond angles, and torsion angles for DiCICA. This material is available free of charge via the Internet at <http://pubs.acs.org>.

References and Notes

- Irie, M.; Kobatake S.; Horichi, M. *Science* **2001**, *291*, 176.
- Chorev, M.; Goodman, M. *Trends Biotechnol.* **1995**, *13* (10), 438.
- Ramos, A.; Techert, S. *Phys. Chem. Chem. Phys.* **2003**, *5*, 5176.
- Hamilton, T. D.; Papaefstathiou, G. S.; MacGillivray, L. R. *J. Solid State Chem.* **2005**, *178*, 2409.
- Collet, E.; Lemée-Cailleau, M.-H.; Buron-Le Cointe, M.; Cailleau, H.; Wulff, M.; Luty T.; Koshihara, S.-Y.; Meyer, M.; Toupet, L.; Rabiller, P.; Techert, S. *Science* **2003**, *300*, 612.
- Techert, S.; Schotte, F.; Wulff, M. *Phys. Rev. Lett.* **2001**, *86*, 2030.
- Busse, G.; Tschentscher, Th.; Plech, A.; Wulff, M.; Frederichs, B.; Techert, S. *Faraday Discuss.* **2003**, *122*, 105.
- Davaasambuu, J. Techert, S. *J. Phys. D: Appl. Physics* **2005**, *38*, A204.
- Techert, S. Zachariasse, K. A. *J. Am. Chem. Soc.* **2004**, *126*, 5593.
- Vorontsov, I. I.; Kovalevsky, A. Y.; Chen, Y.-S.; Graber, T.; Gembicky, M.; Novozhilova, I. V.; Omary, M. A.; Coppens, P. *Phys. Rev. Lett.* **2005**, *94*, 193003.
- Cohen, M. D.; Schmidt, G. M. J. *J. Chem. Soc.* **1964**, 1996.
- Nakanishi, F.; Nakanishi, H.; Tasai, T.; Suzuki Y.; Hasegawa, M. *Chem. Lett.* **1974**, 525.
- Nakanishi, F.; Nakanishi, H.; Tsuchiya M.; Hasegawa, M. *Bull. Chem. Soc. Jpn.* **1976**, *49*, 9 (11), 3096.
- Kaupp, G. *Angew. Chem., Int. Ed. Engl.* **1992**, *31* (5), 592.
- Enkelmann, V.; Wegner, G.; Novak, K.; Wagener, K. B. *J. Am. Chem. Soc.* **1993**, *115*, 10390.
- Cohen, M. D.; Schmidt, G. M. J.; Sonntag, J. *J. Chem. Soc.* **1964**, 2000.
- Thomas, J. M. *Philos. Trans. R. Soc. London* **1974**, *277*, 251.
- Harris, K. D. M.; Thomas, J. M. *J. Solid State Chem.* **1991**, *93*, 197.
- Allen, F. H.; Mahon, M. F.; Raithby, P. R.; Shields, G. P.; Sparkes, H. A. *New J. Chem.* **2005**, *29* (1), 182.
- Hertel, F. Z. *Electrochimica* **1931**, *37*, 536.
- Mustafa, A. *Chem. Rev.* **1951**, *51*, 1.
- Schmidt, G. M. J. *Pure Appl. Chem. Soc.* **1971**, *27*, 647.
- Zimmermann, H. E.; Sebek, P. *J. Am. Chem. Soc.* **1997**, *119*, 3667.
- Zimmermann, H. E.; Sebek, P.; Zhu, Z. *J. Am. Chem. Soc.* **1998**, *120*, 8549.
- Zimmermann, H. E.; Nesterov, E. E. *Acc. Chem. Res.* **2002**, *35*, 77.
- McBride, J. M. *Acc. Chem. Res.* **1983**, *16*, 304.
- Weiss, R. G.; Ramamurthy, V.; Hammond, G. S. *Acc. Chem. Res.* **1993**, *26*, 530.
- Gavezotti, A.; Simonetta, M. *Chem. Rev.* **1982**, *82*, 1.
- Ohashi, Y.; Tomotake, Y.; Akira, U.; Sasada, Y. *J. Am. Chem. Soc.* **1986**, *108*, 1196.
- Ramamurthy, V.; Venkatesan, K. *Chem. Rev.* **1987**, *87*, 433.
- Atkinson, S. D. M.; Almond, M. J.; Hibble, S. J.; Hollins, P.; Jenkins, S. L.; Tobin, M. J.; Wiltshire, K. S. *Phys. Chem. Chem. Phys.* **2004**, *6*, 4.
- Davaasambuu, J.; Durand, P.; Techert, S. *J. Synchrotron Rad.* **2004**, *11*, 483.
- Data Collection and Processing Software for the SMART System, Bruker-AXS Inc., Madison.
- Sheldrick, G. M.; *SHELX97*, Program for the refinement of crystal structures, University of Goettingen: Germany, 1997.
- DiCICA crystallizes in the triclinic space group **P-1** with the lattice parameters: $a = 3.813$ (1) Å, $b = 8.498$ (2) Å, $c = 14.750$ (4) Å, $\alpha = 105.957$ (10)°, $\beta = 93.157$ (7)°, $\gamma = 99.942$ (9)°. The structure was determined in detail and refined by the full-matrix least-squares methods to a final R factor of 3.3% with 1993 independent reflections. Further details on the crystal data for the monomer crystal and the experimental conditions are listed in Table 1 (of Supporting Information) including the numbering of Figure 2 for the molecular structure. The final atomic parameters and isotropic displacement parameters are given in Table 2 (supplement) and a selection of bond lengths, angles, and torsion angles in Table 3 (Supporting Information).
- Techert, S. *J. Appl. Crystallogr.* **2004**, *37*, 445.
- Techert, S.; Schmatz, S. In preparation.
- Hasegawa, M.; Shiba, S. *J. Phys. Chem.* **1982**, *86*, 1490.